ESC European Society of Cardiology

Cardiovascular Research (2022) **118**, 2124–2138
https://doi.org/10.1093/cvr/cvab257

Cardiac natriuretic peptide deficiency sensitizes the heart to stress-induced ventricular arrhythmias via impaired CREB signalling

Eric J. Hall [1†], Soumojit Pal[2†], Michael S. Glennon[2], Puneeth Shridhar [2], Sidney L. Satterfield[2], Beth Weber [2], Qinkun Zhang[3], Guy Salama [2], Hind Lal [3], and Jason R. Becker [2*]

[1]Department of Medicine, Vanderbilt University Medical Center, Nashville, TN, USA; [2]Pittsburgh Heart, Lung, Blood, and Vascular Medicine Institute and Division of Cardiology, Department of Medicine, University of Pittsburgh School of Medicine and University of Pittsburgh Medical Center, Pittsburgh, PA, USA; and [3]Division of Cardiovascular Disease, Department of Medicine, University of Alabama at Birmingham Medical Center, Birmingham, AL, USA

Received 12 April 2021; editorial decision 25 July 2021; accepted 28 July 2021; online publish-ahead-of-print 30 July 2021

Aims The cardiac natriuretic peptides [atrial natriuretic peptide (ANP) and B-type natriuretic peptide (BNP)] are important regulators of cardiovascular physiology, with reduced natriuretic peptide (NP) activity linked to multiple human cardiovascular diseases. We hypothesized that deficiency of either ANP or BNP would lead to similar changes in left ventricular structure and function given their shared receptor affinities.

Methods and results We directly compared murine models deficient of ANP or BNP in the same genetic backgrounds (C57BL6/J) and environments. We evaluated control, ANP-deficient (Nppa-/-) or BNP-deficient (Nppb-/-) mice under unstressed conditions and multiple forms of pathological myocardial stress. Survival, myocardial structure, function and electrophysiology, tissue histology, and biochemical analyses were evaluated in the groups. *In vitro* validation of our findings was performed using human-derived induced pluripotent stem cell cardiomyocytes (iPS-CMs). In the unstressed state, both ANP- and BNP-deficient mice displayed mild ventricular hypertrophy which did not increase up to 1 year of life. NP-deficient mice exposed to acute myocardial stress secondary to thoracic aortic constriction (TAC) had similar pathological myocardial remodelling but a significant increase in sudden death. We discovered that the NP-deficient mice are more susceptible to stress-induced ventricular arrhythmias using both *in vivo and ex vivo* models. Mechanistically, deficiency of either ANP or BNP led to reduced myocardial cGMP levels and reduced phosphorylation of the cAMP response element-binding protein ($CREB^{S133}$) transcriptional regulator. Selective CREB inhibition sensitized wild-type hearts to stress-induced ventricular arrhythmias. ANP and BNP regulate cardiomyocyte $CREB^{S133}$ phosphorylation through a cGMP-dependent protein kinase 1 (PKG1) and p38 mitogen-activated protein kinase (p38 MAPK) signalling cascade.

Conclusions Our data show that ANP and BNP act in a non-redundant fashion to maintain myocardial cGMP levels to regulate cardiomyocyte p38 MAPK and CREB activity. Cardiac natriuretic peptide deficiency leads to a reduction in CREB signalling which sensitizes the heart to stress-induced ventricular arrhythmias.

*Corresponding author. Tel: +1 412 648 2358; fax: +1 412 648 5980, E-mail: beckerj@pitt.edu
†The first two authors contributed equally to the study.

Graphical Abstract

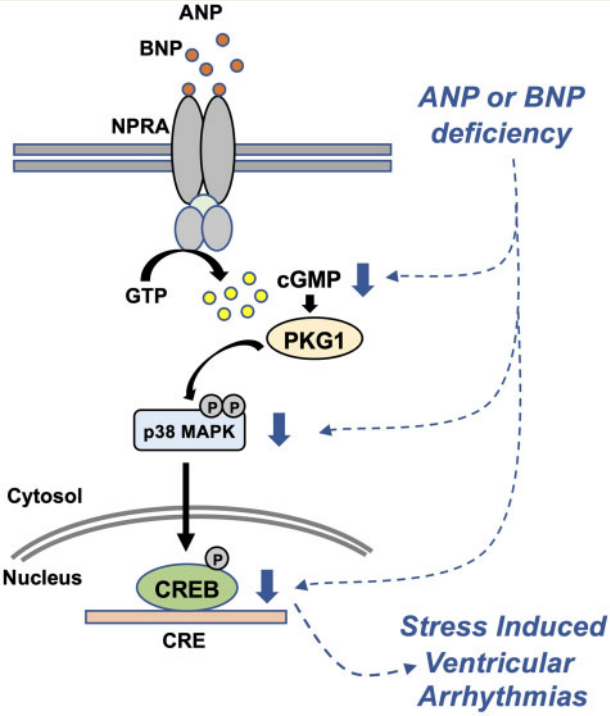

Keywords Heart failure • Sudden death • Natriuretic peptide • Ventricular arrhythmias • Stress

1. Introduction

The cardiac natriuretic peptides represent a highly conserved family of signalling molecules released by the heart in response to cardiac stress, including chamber distension, heart failure, and myocardial ischaemia.[1–3] Cardiac natriuretic peptides (NPs) are known to play an important role in regulating volume status, vasodilation, and sympathetic activation.[4–7] The primary natriuretic peptides produced by the heart are atrial natriuretic peptide (ANP) and B-type natriuretic peptide (BNP), which are encoded by the genes Nppa and Nppb, respectively.[8] ANP and BNP exert their primary effects through binding the guanylyl-cyclase-linked receptor Npr1. Receptor activation leads to production of cyclic guanosine 3'5'-monophosphate (cGMP) which in turn can activate cGMP-dependent protein kinase isoforms (PKG1 or PKG2).[7,9] Evidence suggests that ANP affinity for Npr1 is equal to or greater than BNP affinity for Npr1.[10,11] ANP and BNP are cleared through two primary mechanisms. The first mechanism is mediated by a receptor known as Npr3 which binds natriuretic peptides and removes them by way of receptor-mediated endocytosis.[12,13] A second means of NP clearance occurs through proteolytic degradation by an extracellular protease known as neprilysin.[12,14]

Natriuretic peptide deficiency (quantitative or functional deficiency) has been linked to the development of multiple cardiovascular disease states in humans, including hypertension, atrial fibrillation, and cardiac hypertrophy.[15–17] Natriuretic peptide levels are lower in Black patients and in obese patients, a finding which may predispose to the development of cardiovascular disease.[18,19] Likewise, humans with heart failure have elevated natriuretic peptides.[20] However, clinical evidence suggests human heart failure is actually characterized by an effective NP deficiency, due to predominantly biologically inactive NP forms.[21–23] Furthermore, neprilysin inhibition (in conjunction with angiotensin-receptor blockade) has emerged as a new class of heart failure treatment, demonstrating significantly reduced mortality.[24] Prior research has shown loss of ANP in a murine model leads to mild cardiac hypertrophy and salt-sensitive hypertension,[25–27] and a BNP-deficient mouse was reported to have increased cardiac fibrosis.[28] However, a direct comparison of ANP- and BNP-deficient mice in similar genetic backgrounds has not been performed. In addition, despite the potential importance of NP deficiency in human heart failure, mechanisms of how ANP and BNP modify cardiomyocyte signalling pathways remain incompletely understood.

As both ANP and BNP act through the same receptors, we hypothesized that deficiency of ANP or BNP would lead to similar effects on myocardial structure and function. To test this hypothesis, we directly compared the effect of ANP or BNP deletion on left ventricular (LV) remodelling in an effort to understand how these peptides regulate the cardiomyocyte response to pathological stress. We then utilized human-derived iPS-CM to further refine the mechanism through which ANP and BNP modify cardiomyocyte signalling pathways. These findings are particularly important given the expanding role of modulating natriuretic peptides in the treatment of human heart failure.

2. Methods

2.1 Murine models

All murine models were used in a C57/BL6J genetic background and bred on this background for a minimum of six generations before experiments were performed. ANP-deficient (Nppa-/-) mice were obtained from the Jackson Laboratory (JAX stock #002685).[25] BNP-deficient (Nppb-/-) mice were obtained from the KOMP Repository of the Knockout Mouse Project ($Nppb^{tm1(KOMP)Mbp}$, Project ID CSD69054) and crossed with CMV-cre (JAX stock 006054) mice to remove the Neo cassette. The murine model of Mybpc3 deficiency (Mybpc3-Tm1d) was previously described.[29] All mice were maintained on a 0.39% sodium diet (PicoLab Laboratory Rodent Diet 5L0D) and were housed together in groups of up to five mice. Both male and female mice were used, and genetically modified mice were compared to wild-type (WT) littermates.

2.2 Echocardiography

Transthoracic echocardiography was performed using a Vevo2100 or Vevo3100 system (VisualSonics, Inc.). Two-dimensional M-mode images were obtained in conscious mice that had been acclimated to the ultrasound procedure. From these images, parameters including interventricular septal thickness at end diastole (IVSd), left ventricular posterior wall thickness at end diastole (LVPWd), left ventricular internal diameter at end diastole (LVIDd), and left ventricular internal diameter at end systole (LVIDs) were obtained. LV fractional shortening was calculated using the formula (LVIDd–LVIDs)/LVIDd. Diastolic functional assessment was obtained in sedated mice using 3% isoflurane for induction and 1.5% isoflurane for maintenance with adjustment to keep the average heart rate 400–450 b.p.m. Mitral flow velocities during early (E wave) and late (A wave) phases of diastole were obtained by Doppler interrogation of the mitral orifice. All images were obtained and assessed by an individual blinded to genotype.

2.3 Blood pressure measurement

Blood pressures were measured at 2 and 6 months of age using non-invasive tail-cuff measurements. At 6 months of age, a CODA non-invasive tail-cuff blood pressure system was used (Kent Scientific Corporation). Blood pressures were checked at the same time over 3 days to acclimate the mice, and final measurements were recorded on Day 3. Mice were warmed to 37°C while being measured. A minimum of 10 measurements were averaged per animal for systolic blood pressure. Blood pressures were also measured on 2-month-old mice using a BP2000 tail-cuff system (Visitech Systems), using an average of at least three measurements per mouse.

2.4 Transverse aortic constriction

TAC was performed as previously described.[30] Two-month-old mice were sedated with isoflurane (3% for induction, 1.5% for maintenance) and then injected with intraperitoneal ketamine (100 mg/kg) for anaesthesia. Aortic constriction was performed by tying a 7-0 nylon suture ligature against a 27-gauge needle. The needle was promptly removed to yield a constriction of ~0.4 mm. All mice were operated on by the same surgeon who was blinded to genotype. Transaortic gradient was measured in sedated mice one week after surgery using the Vevo 2100 ultrasound system (Supplementary material online, *Figure S1A–C*). Flow velocity across the aortic constriction was obtained using pulse-wave Doppler interrogation distal to the constriction. The transaortic gradient was calculated from the flow velocity using the modified Bernoulli equation. The average transaortic gradient was similar across WT, Nppa-/-, and Nppb-/- utilized for subsequent comparisons (Supplementary material online, *Figure S1D*). Six weeks after TAC, mice underwent echocardiography and were then euthanized to determine heart weight and tibia length.

2.5 Euthanasia and heart mass assessment

Mice were sedated with continuous infusion of 5% isoflurane (Henry Schein) using nose cone. Once unresponsive to toe pinch, total body weight was obtained, and the heart was then removed. The heart was perfused with 0.5 M KCl prior to obtaining heart weight. The chest cavity was examined for signs of infection or haemorrhage. Mouse lower extremities were amputated at the proximal femur and then boiled to remove all soft tissues. After the tibia was cleaned and isolated, tibia length was measured with digital calipers. Heart weight-to-tibia length (mg/mm, HW/TL) ratios were then calculated.

2.6 Histologic analysis

To determine fibrotic area, fresh-frozen 10-μm sections were obtained from OCT-embedded tissue and fixed with acetone for 10 min at -20°C. Sections were allowed to air-dry for 20 min and then rehydrated with a 1× PBS wash for 1 min. Following this, sections were submerged in Sirius Red/Fast Green staining solution (Chondrex 90461) for 60 min, followed by a rinse with distilled water. A Zeiss Axioplan 2 microscope was then used to obtain bright-field images of the tissue at 20×. These images were analysed using ImageJ software. The total myocardial area was measured, which included both green- and red-stained tissue. Then only the fibrotic area was measured (Sirius Red positive only). The ratio of Sirius Red tissue area to total tissue area was then calculated to obtain the percentage of fibrotic area per myocardial tissue section. A minimum of 15 images per tissue sample were measured.

2.7 Murine electrocardiography

The C57BL/6J age-matched control mice, Nppa-/-, and Nppb-/- mice were anaesthetized with 50 mg/kg ketamine/5 mg/kg xylazine via intraperitoneal injection. Once anaesthesia was established, a 2-min baseline EKG was obtained and the mice were then administered 1.5 mg/kg of isoproterenol (Sigma I6504) by intraperitoneal injection. Cardiac rhythm was then continuously recorded for an additional 30 min after injection using ADInstruments PowerLab and Bio Amp. All EKG rhythm data were analysed by an individual blinded to genotype using LabChart Reader (ADInstruments, v8.1.8). PR interval was measured from the start of the P wave to the beginning of the QRS complex. The QRS duration was defined as starting at the first deflection following the P wave to the halfway point of the S-peak and J-wave peak.[31] QT interval was measured according to the method of Zhang *et al.*,[32] from the start of QRS activation to the trough of the T wave. In accordance with the updated Lambeth Conventions, a premature ventricular complex (PVC) was defined as a ventricular electrical complex which was abnormal and premature in the context of the baseline EKG morphology.[33] Non-sustained ventricular tachycardia was defined as at least three consecutive abnormal ventricular complexes. Sustained ventricular tachycardia was defined as consecutive ventricular complexes lasting 30 s or greater.

2.8 *In vivo* CREB inhibition

The selective CREB inhibitor, 666-15[34] (5661, Tocris), was dissolved in DMSO to a stock concentration of 50 mg/mL. The stock solution was

then diluted in sesame oil to a 10 mg/kg final concentration with a final DMSO concentration of 2% or less. Three-month-old C57BL/6J mice were then administered 666-15 (10 mg/kg) or vehicle (DMSO 2%+sesame oil) via intraperitoneal injection (IP) for 16 consecutive days. The vehicle and CREB inhibitor groups were then anaesthetized with 1% isoflurane using nose cone and a baseline 2-min EKG was obtained. After the baseline EKG, 1.5 mg/kg of isoproterenol (Sigma I6504) was administered by intraperitoneal injection. Cardiac rhythm was then continuously recorded for 30 min. EKG analysis was performed as outlined in the murine electrocardiography section.

2.9 Optical mapping

Mice were anaesthetized with Euthasol (96 mg/kg) and injected with heparin (35 mg/kg). The heart was excised and perfused on a Langendorff apparatus with physiological Tyrode's solution containing 112 mM NaCl, 1.8 mM $CaCl_2$, 5 mM KCl, 1.2 mM $MgSO_4$, 1 mM KH_2PO_4, 25 mM $NaHCO_3$, and 50 mm D-glucose at pH 7.4. The solution was continuously bubbled with 95% O_2 and 5% CO_2. The hearts were then stained with bolus injections of a voltage-sensitive dye and a Ca^{2+} indicator, RH237 and Rhod-2/AM, respectively.[35] Light was collimated, passed through 530 ± 30 nm interference filters, split by a 560 nm dichromatic mirror, and focused on the heart. Fluorescence from the heart was collected with tandem camera lenses and was split with a 600 nm dichroic mirror to focus the images at short (570–595 nm) and long (610–750 nm) wavelengths on two CMOS cameras (SciMedia, Ultima One). Each camera (100 × 100 pixels) viewed a 4 × 4 mm^2 area of the anterior surface of the heart and was scanned at 1000 frames/s.[36] The spatial and temporal resolution was 400 μm/pixel and 1 ms, respectively. To test arrhythmia vulnerability, each heart was paced at the ventricle using a programmed stimulation protocol. The protocol ranged from 40 pulses, 2 ms duration, 60 ms interval to 100 pulses, 2 ms duration, 20 ms interval.

2.10 Plasma NP measurement

Whole blood samples from 1-month-old Nppa-/-, Nppb-/-, and WT mice were obtained by cardiac puncture and collected in pre-cooled tubes containing Na2-EDTA. Plasma was separated by centrifugation at 4000 × *g* for 10 min at 4°C and stored at –80°C before analysis. ANP and BNP were measured from plasma using ANP (catalogue FEK-005-24) and BNP-45 (catalogue FEK-011-23) Fluorescent Immunoassay kit (Phoenix Pharmaceutical, Burlingame, CA, USA), respectively, according to the manufacturer's instruction. Concentration of peptides (ANP and BNP) was determined from respective standard curves and expressed as pmol/mL.

2.11 qPCR

Total RNA from mouse left ventricular tissue underwent reverse transcription (QuantiTect Reverse Transcription Kit, Qiagen, Hilden, Germany) to generate first-hand cDNA according to manufacturer's protocol. To perform gene expression analysis, qRT-PCRs were set up in a Quant-Studio-5 Real-Time PCR System (Applied Biosystems) using SYBR Green Reagent (Thermo Fisher Scientific) and gene-specific primers (Supplementary material online, *Table S1*). Each sample was run in triplicate, and the CT value was normalized using endogenous housekeeping gene Rpl32. The $2^{-\Delta\Delta Ct}$ method was used to calculate the fold change in mRNA expression relative to indicated group and represented in log scale in figure legends. Genes with CT values >35 were considered undetectable.

2.12 cGMP measurement

Cyclic nucleotides were quantified from the flash-frozen (using liquid nitrogen) left ventricle myocardial tissue from 1-month-old Nppa-/-, Nppb-/-, or WT mice. Frozen tissue was homogenized into 10 volumes (mL of solution/gram of tissue) of 5% trichloroacetic acid (TCA) (catalogue T0699, Sigma) and centrifuged at 1500 × *g* for 10 min at 4°C. Supernatants collected in fresh tubes were washed with water-saturated ether (catalogue 309966, Sigma) for two times. After removal of the residual ether by heating the sample to 70°C for 5 min, the cGMP level was measured using competitive enzyme immunoassay (EIA) kit according to the manufacturer's protocol (catalogue 581021, Cayman Chemicals). Standards and samples from each group were assayed in triplicate, and each sample was assayed at two different dilutions. Absorbance measurements were expressed as % binding using the formula [(Bi - NSB/B0-NSB) × 100], where Bi represented the binding of samples or standards; B0 is the maximum binding and NSB is the non-specific binding. Concentration of the analytes (cGMP) was determined from the standard curves and expressed as fmol/mg tissue.

2.13 Human cardiomyocytes derived from induced pluripotent stem cells

Human-induced pluripotent stem cells (hiPSCs) were obtained from the Stanford SCVI BioBank (SCVI13 and SCVI274) and differentiated into human iPSC cardiomyocytes (human iPS-CM) according to a modified version of the protocol developed by Burridge *et al.*[37] In brief, hiPSCs were grown on six-well tissue culture dishes coated with growth factor-reduced Matrigel (Corning, 354230) in essential 8™ Medium (Gibco). Confluent cells (~80%) were treated with RPMI 1640 media supplemented with B27 minus insulin (Gibco) and 10 μM CHIR99021 (Selleckchem). After 48 h, media were switched to RPMI 1640 with B27 minus insulin and 5 μM IWR-1 (Sigma) for again 48 h. Media were then switched to RPMI 1640 with B27 minus insulin every other day until differentiated cells (hiPS-CM) started contracting at Day 7 post-differentiation. At post-differentiation Day 10, iPSC-CMs were selected by treating with RPMI 1640 without glucose which had been supplemented with Sodium L-lactate (Sigma).[38] At post-differentiation Day 15, cells were given RPMI 1640 with glucose and ITS plus media supplement (AR014, R&D Systems) every other day until Day 30 post-differentiation and used for experiments. The purity of hiPS-CMs was checked through α-actinin staining (>95%). Cultures were maintained in a humidified atmosphere with 5% CO_2 at 37°C. hiPS-CMs were treated with ANP (AS-20648, Anaspec), BNP (AS-24015, Anaspec), or 8-Bromo-cGMP (15992, Cayman Chemicals) for 2 h. For inhibitor experiments, hiPS-CMs were pre-treated either with KT 5823 (10010965, Cayman Chemicals), SB203580 (S1076, Selleckchem), GDC-0994 (S7554, Selleckchem), or with 666-15 (5661, Tocris) followed by ANP treatment.

2.14 siRNA transfection

For transfection experiment, 1 × 10^5 hiPS-CMs (30–35 days post-differentiation) were seeded onto a 12-well plate. Silencer Select Predesigned siRNA (Thermo Fisher Scientific) for PRKG1 (Ambion; ID: S11133) or negative control siRNA (Ambion; Cat: AM4611) to a final concentration of 100 nM was introduced into culture medium using Lipofectamine® RNAiMAX Transfection Reagent (Thermo Fisher Scientific) according to the manufacturer's protocol. Both siRNAs and RNAiMAX were diluted with Opti-MEM® reduced serum medium (Life Technologies) before introduction into the cells. Media were refreshed

every 48 h with new siRNA:RNAiMAX mixture. After 8 days of transfection, cells were incubated with ANP for 2 h and harvested using RIPA lysis buffer containing protease/phosphatase inhibitors for western blot analysis.

2.15 Electrophoresis and western blot analysis

Left ventricular cardiac tissue or hiPS-CMs were homogenized in ice-cold RIPA buffer (Thermo Fisher Scientific, 89900) containing protease/phosphatase inhibitors (Thermo Fisher Scientific, 78441). Supernatant was separated by centrifugation at 14 000 × *g* for 20 min at 4°C and stored at -80°C until further use. Proteins (50 µg/lane) were resolved through SDS–PAGE using 10% Tris–HCl gel (Criterion TGX precast gel, Bio-Rad) and transferred to a 0.45-µm low-fluorescence PVDF membrane (Bio-Rad) at 100 V for 60 min at 4°C using wet/tank blotting system apparatus (Bio-Rad). Membranes were subsequently blocked with intercept (TBS) blocking buffer (Licor Biotech) or 5% BSA in TBS containing 0.1% Tween-20 (TBST) and probed with primary antibody targeting phospho-CREB (Ser133) (catalogue 9198), CREB (catalogue 9104), phospho-p38 MAPK (Thr180/Tyr182) (catalogue 4511), p38 MAPK (catalogue 8690), GAPDH (catalogue 5174) (all from Cell Signaling Technology), CREM (catalogue ARP34778_P050 from Aviva Systems Biology), and PKG1 (catalogue ADI-KAP-PK005 from Enzolifescience) antibodies overnight at 4°C. Membranes were washed with TBST and subsequently incubated with IRDye 680 LT (goat anti-mouse or anti-rabbit) or IRDye 800 CW (goat anti-mouse or anti-rabbit) for 1 h at room temperature, and imaging was done on an Odyssey CLx imaging system (Licor Biotech). Membranes were subsequently stripped (NewBlot IR stripping buffers, Licor Biotech) and reprobed for detection of loading proteins. For chemiluminescent detection, goat anti-rabbit HRP was used, and images were recorded in Chemi Doc apparatus (Bio-Rad). Band intensities of blots were then analysed using Image Studio Lite (Licor Biotech) and Image J Software.

2.16 Immunocytochemistry

For detection of CREB activation and its localization, hiPS-CMs (1×10^4 cells/well) were plated on sterile chamber slides (Corning). Following treatments, cells were rinsed with 1X PBS and fixed in 4% paraformaldehyde for 15 min at room temperature (RT). After washed (x3) with 1XPBS, cells were permeabilized with PBS + 0.5% triton-X-100 for 15 min followed by incubation with blocking solution (1% BSA in PBS) for 1 h at RT. Cells were then incubated with primary antibodies targeting phospho-CREB (catalogue 9198, CST) and sarcomeric α-actinin (catalogue ab9465, Abcam) in blocking buffer overnight at 4°C. The following day, cells were washed and incubated with fluorescent secondary goat anti-rabbit Alexa Fluor 594 (catalogue A-11005, Thermo Fisher Scientific) and goat anti-mouse Alexa Fluor 488 (catalogue A-10667, Thermo Fisher Scientific) antibodies for 1 h at room temperature. After final PBS washes, cells were mounted with ProLong Gold Antifade with DAPI (Thermo Fisher Scientific) and allowed to cure overnight in the dark. Slides were then visualized and imaged under wide-field fluorescent microscope (Zeiss) at 100X magnification with oil.

2.17 Statistics

All data are displayed as mean ± SEM unless otherwise noted. Data were analysed using a two-tailed unpaired Student's *t*-test for equal variances and Welch's *t*-test for unequal variances to make comparisons between two groups involving continuous variables. Categorical variables were analysed using a chi-square test. A log-rank (Mantel–Cox) test was performed to analyse survival curves. Significance was defined as $P < 0.05$. Statistical analyses were performed using GraphPad Prism version 8.4.2 (GraphPad Software, San Diego, CA, USA).

2.18 Study approval

All animal protocols and procedures were performed in accordance with NIH guidelines and approved by the Institutional Laboratory Animal Care and Use Committee at Vanderbilt University Medical Center and University of Pittsburgh. Human iPS cell lines were derived from consented research subjects in the Stanford SCVI BioBank, and the cell lines were distributed in a deidentified manner to the investigators. This study conformed to the principles outlined in the Declaration of Helsinki.

3. Results

3.1 Chronic natriuretic peptide deficiency causes mild LV structural defects in the unstressed state

We first examined WT, Nppa-/-, and Nppb-/- animals in the unstressed state. We phenotyped cohorts of mice at multiple time points (1, 2, 6, and 12 months old) using echocardiography and tissue analysis. We observed mild structural differences in NP-deficient mice at younger ages which were stable or diminished with aging (*Figure 1A–D*). At 2 months of age, both Nppa-/- and Nppb-/- mice exhibited slightly increased septal and left ventricular posterior wall thickness relative to WT mice (*Figure 1A and B*, Supplementary material online, *Table S2*). Nppb-/- mice also had mild LV dilation relative to WT animals at 2 months, but this was not apparent at later ages (*Figure 1C*). In addition, Nppa-/- animals displayed increased overall cardiac mass relative to Nppb-/- and WT mice at 2 and 6 months (*Figure 1D*). However, by 12 months of age, there were minimal differences in myocardial mass between WT and either NP-deficient model. Left ventricular myocardial fibrosis was also assessed and was significantly increased in Nppa-/- but interestingly not Nppb-/- animals at 6 months of age (*Figure 1E and F*).

We saw minimal changes in left ventricular systolic function at all ages assessed (*Figure 1G*). In addition, there was no statistical difference in left ventricular diastolic function (as assessed by *E/A* ratio and deceleration time) across the three genotypes but there was a trend to increased *E/A* ratio in Nppa-/- animals (*Figure 1H and I*). Nppa+/- and Nppb+/- heterozygous animals did not exhibit differences in LV structure or systolic function compared to control WT mice (Supplementary material online, *Table S2*). We also analysed if there were detectable gender differences between the groups (Supplementary material online, *Figure S2C–H*). The primary difference we detected was slightly less LV hypertrophy in female mice deficient in ANP or BNP compared to male mice deficient in ANP or BNP (Supplementary material online, *Figure S2C and D*). Lastly, we did not observe a significant difference in systolic blood pressure across the three genotypes at multiple ages in mice fed a standard chow diet (0.39% salt diet) (*Figure 1J*).

3.2 Natriuretic peptide deficiency does not alter left ventricular remodelling following thoracic aortic constriction

Next, we wanted to determine if chronic NP deficiency altered pathological left ventricular remodelling secondary to an acute increase in

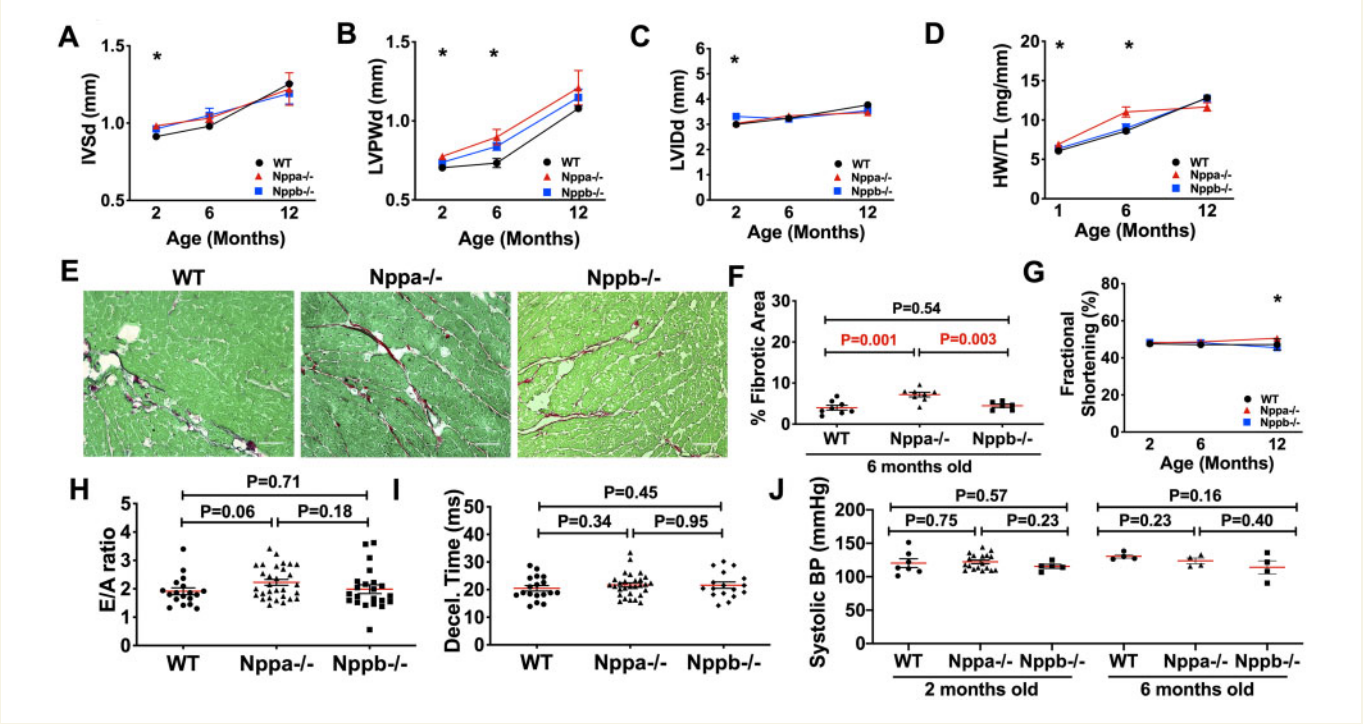

Figure 1 Chronic natriuretic peptide deficiency causes mild LV structural defects in the unstressed state. (*A*) Echocardiographic assessment of interventricular septal diameter at end diastole (IVSd, mm). *$P < 0.05$ Nppa-/- vs. WT 2 months. (*B*) Left ventricular posterior wall thickness at end diastole (LVPWd, mm) * $P < 0.05$ Nppa-/- vs. WT at 2 and 6 months, Nppb-/- vs. WT at 6 months. (*C*) Left ventricular internal diameter at end diastole (LVIDd, mm). *$P < 0.05$ Nppb-/- vs. WT 2 months, or Nppb-/- vs. Nppa-/- 2 months. Samples sizes: $N = 24$–34/group (2 months), $N = 9$/group (6 months), $N = 4$–6/group (12 months). (*D*) Heart weight to tibia length (HW/TL, mg/mm) at 1 month ($N = 5$–10/group), 6 months (6–10/group), and 12 months of age ($N = 4$–6/group). *$P < 0.05$ Nppa-/- vs. WT 2 and 6 months. (*E*) Representative images of LV myocardial fibrosis as assessed by Sirius Red/Fast Green staining in each genotype at 6 months of age. Scale bar = 50 μM. (*F*) Per cent fibrotic area among WT, Nppa-/-, and Nppb-/- animals ($N = 6$–8/group). (*G*) Conscious echocardiography measurement of LV systolic function as assessed by LV fractional shortening percentage in WT, Nppa-/-, and Nppb-/- mice at 2, 6, and 12 months of age. *$P < 0.05$ Nppa-/- vs. WT or Nppb-/- at 12 months of age. Samples sizes $N = 24$–34/group (2 months), $N = 9$/group (6 months), $N = 4$–6/group (12 months). (*H* and *I*) LV diastolic function as assessed by anesthetized echocardiography to measure early (*E*) to late (*A*) left ventricular filling velocities expressed as *E*/*A* ratio (*H*) and deceleration time (*I*, ms) at 2 months of age ($N = 18$–30/group). (*J*) Systolic blood pressure at 2 months ($N = 5$–18/group) and 6 months of age ($N = 4$/group). Student's *t*-test used to assess means between two groups. Data shown as means ± SEM.

myocardial afterload induced by thoracic aortic constriction (TAC). Six weeks after TAC, all three genotypes of mice exhibited a mild decrease in systolic function with an increase in myocardial hypertrophy as assessed by wall thickness measurements and heart mass (*Figure 2A and B*, Supplementary material online, *Table S3*). Nppa-/- mice had increased septal thickness at 2 months of age at baseline and remained statistically different after TAC (*Figure 2A*). Likewise, Nppb-/- mice had increased left ventricular diastolic diameter at baseline, and this remained statistically different after TAC (*Figure 2A*). There was a trend of increased cardiac mass in the Nppa-/- and Nppb-/- mice after TAC compared to WT mice, but it was not statistically significant (*Figure 2B*). Similar to the unstressed state, Nppa-/- mice exhibited the highest level of left ventricular fibrosis compared to WT and Nppb-/- mice after TAC (*Figure 2C and D*).

Since Nppa-/- and Nppb-/- mice had structural abnormalities pre-TAC (*Figure 1*), we calculated the per cent change from pre- to post-TAC for each mouse across the three genotypes. This allowed us to more directly evaluate if deficiency of either ANP or BNP modified left ventricular function and remodelling after TAC. Interestingly, the per cent change from pre- to post-TAC in left ventricular hypertrophy (*Figure 2E and F*), left ventricular dilation (*Figure 2G*), and systolic function (*Figure 2H*) was not significantly different across genotypes. Therefore, deficiency of ANP or BNP does not appear to dramatically modify left ventricular remodelling after an acute increase in LV afterload induced by TAC.

3.3 Deficiency of either ANP or BNP leads to increased sudden death following an acute increase in myocardial afterload

Left ventricular remodelling after TAC was minimally affected by deficiency of ANP or BNP. In contrast, there was a dramatic increase in early mortality in ANP- or BNP-deficient mice following an acute increase in myocardial afterload (*Figure 3A*). Compared to ANP- or BNP-deficient mice, there was minimal mortality in either WT or ANP or BNP heterozygote mice. Importantly, necropsy detected no evidence of infection or haemorrhage in post-TAC mice that died suddenly. In addition, the TAC surgery was performed in a blinded fashion with all genotypes mixed together. Sudden death in ANP- or BNP-deficient TAC mice occurred at less than 5 days post-operatively and occurred in both female and male

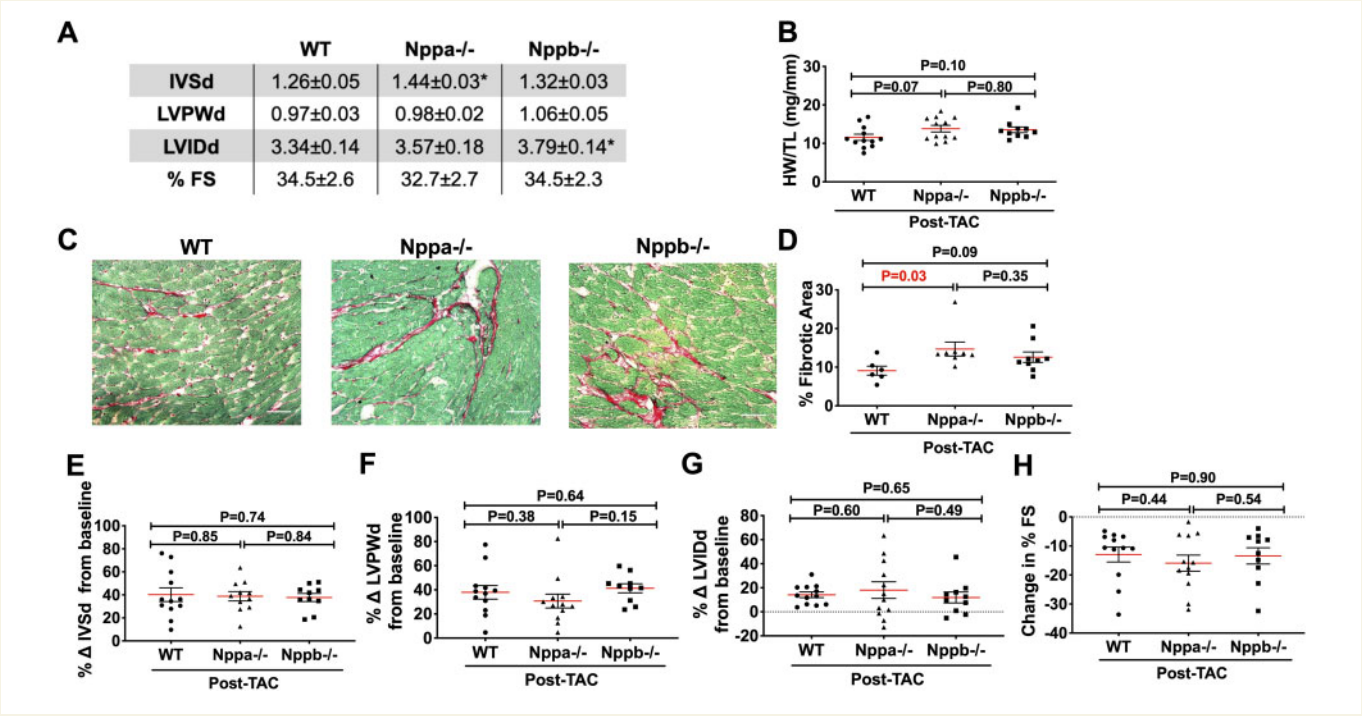

Figure 2 Natriuretic peptide deficiency does not alter left ventricular remodelling following thoracic aortic constriction. (*A*) Six weeks post-TAC conscious echocardiographic measurements of interventricular septal diameter at end diastole (IVSd, mm), left ventricular posterior wall thickness at end diastole (LVPWd, mm), left ventricular internal diameter at end diastole (LVIDd, mm), LV fractional shortening (FS, %), ($N = 10–12$/group). *$P < 0.05$ vs. WT. (*B*) Cardiac mass (HW/TL ratio, mg/mm) at 6 weeks post-TAC. (*C*) Representative images of LV myocardial fibrosis as assessed by Sirius Red/Fast Green staining in each genotype 6 weeks post-TAC. Scale bar = 50 μM. (*D*) LV myocardial fibrotic area (%) ($N = 6–9$/group). (*E–H*) The per cent change from baseline echocardiographic measurements pre-TAC to 6 weeks post-TAC for (*E*) interventricular septal diameter at end diastole (IVSd), (*F*) LV posterior wall thickness at end diastole (LVPWd), (*G*) LV internal diameter at end diastole (LVIDd), (*H*) LV fractional shortening (FS %) change from pre-TAC, ($N = 10–12$/group). Student's *t*-test used to assess means between two groups. Data shown as means ± SEM.

mice (Nppa-/- mice: four males deceased, two females; Nppb-/- mice: five males, four females).

Given the surgical blinding and similar transaortic gradients among survivors of all genotypes (Supplementary material online, *Figure S1*), we do not think the sudden death in the ANP- or BNP-deficient animals was secondary to higher levels of aortic constriction. Another possibility was that TAC sudden death animals exhibited worse cardiac phenotypes prior to surgery compared to the animals that survived TAC. We compared the pre-surgery echoes of both TAC survivors and TAC sudden death mice (*Figure 3B–G*). We observed no difference in LV wall thickness, LV dilation, and LV systolic or diastolic function between TAC survivors and TAC sudden death groups for a given genotype. Therefore, there were no detectable pre-surgery LV structural or functional differences between the TAC survivors and TAC sudden death groups. This data suggests NP deficiency sensitizes the myocardium to acute increases in afterload through a mechanism independent of overt myocardial structural changes.

3.4 ANP or BNP deficiency does not alter survival or LV remodelling in a chronic form of cardiomyopathy

We detected increased sudden death in ANP or BNP mice following an acute increase in left ventricular afterload by TAC. Since TAC is a rapid form of left ventricular hypertrophy and cardiomyopathy we wanted to determine if ANP or BNP deficiency would modify survival or left ventricular remodelling in a chronic form of cardiomyopathy. Therefore, we crossed the Nppa-/- and Nppb-/- mice with mice deficient in myosin binding protein 3 (Mybpc3-/-). Mybpc3-/- mice are a model of a genetic form of human sarcomeric cardiomyopathy and develop evidence of myocardial hypertrophy, left ventricular dilation, and reduced systolic function after birth.[29] In contrast to ANP and BNP mice that underwent TAC, Mybpc3-/- mice deficient in ANP or BNP did not experience any sudden death over a 6-month period of observation. In addition, NP deficiency did not have a significant effect on left ventricular function, myocardial hypertrophy, or myocardial fibrosis in Mybpc3-/- animals at 6 months of age (Supplementary material online, *Figure S3A–G*). ANP or BNP deficiency appears to have minimal effects on pathological left ventricular remodelling in both acute (TAC) or chronic (Mybpc3-/-) forms of cardiomyopathy. In contrast, ANP or BNP deficiency leads to divergent effects on sudden death susceptibility depending on the pathological stimulus (acute TAC vs. chronic Mybpc3 deficiency).

3.5 ANP or BNP deficiency increases susceptibility to ventricular arrhythmias following acute stress

We hypothesized natriuretic peptide deficiency may predispose the heart to ventricular arrhythmias after acute stress because of the increased sudden death in ANP- and BNP-deficient animals after acute

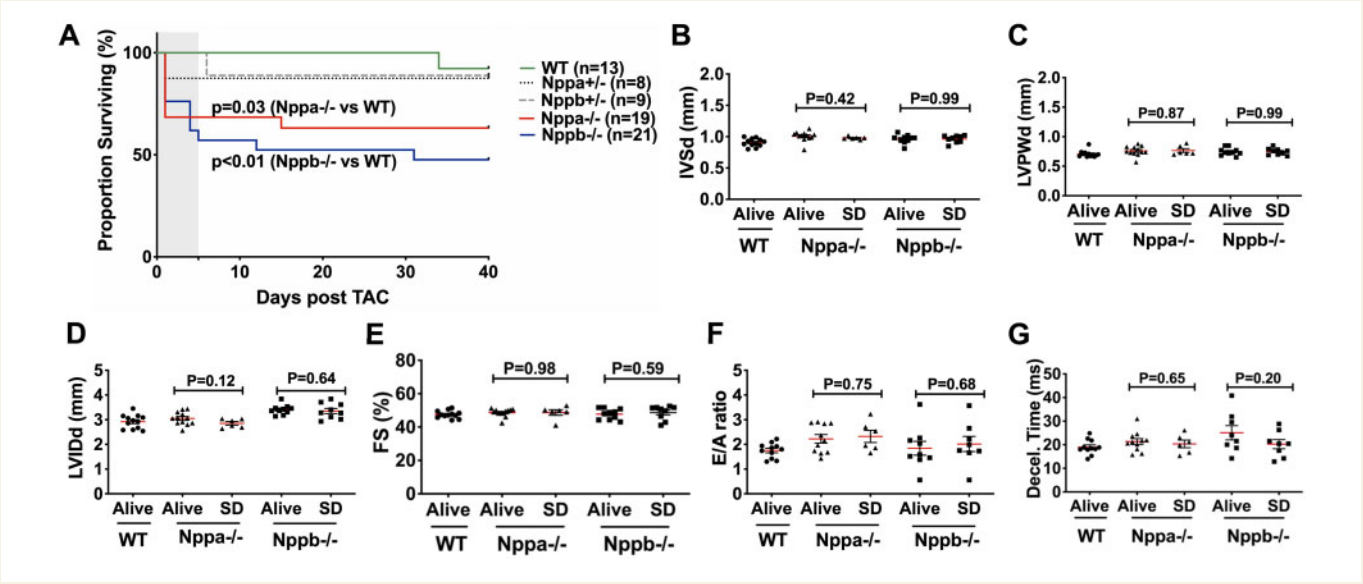

Figure 3 Deficiency of either ANP or BNP leads to increased sudden death following an acute increase in myocardial afterload. (*A*) Survival following TAC for all genotypes. The log-rank (Mantel–Cox) test was used to calculate the difference in survival relative to wild-type mice; statistics shown for survival 5 days post-TAC. (*B–G*) Comparison of baseline pre-TAC echocardiographic measures between survivors and non-survivors (SD = sudden death). (*B*) Interventricular septal diameter at end systole (IVSd, mm). (*C*) LV posterior wall thickness at end diastole (LVPWd, mm). (*D*) LV internal diameter at end diastole (LVIDd, mm). (*E*) LV fractional shortening (FS, %). (*F*) *E/A* ratio. (*G*) deceleration time (ms) ($N = 6–12$/group). Student's *t*-test used to assess means between two groups. Data shown as means ± SEM.

TAC. To test this hypothesis, we first performed continuous EKG monitoring before and after isoproterenol infusion (*Figure 4A*). At baseline there was no significant difference in standard EKG intervals between WT, Nppa-/- or Nppb-/- mice (*Figure 4B*). However, we found that Nppa-/- and Nppb-/- mice had increased premature ventricular contractions (PVC), PVC couplets, and ventricular tachycardia (VT) following isoproterenol infusion (*Figure 4C*). There was no evidence that differences in cardiac mass or LV fibrosis contributed to the increased VT in the Nppa-/- and Nppb-/- animals (*Figure 4D and E*). To exclude potential systemic confounders that may influence VT susceptibility, we performed *ex vivo* analysis of hearts from WT, Nppa-/-, and Nppb-/- animals. We observed that WT hearts did not experience ventricular tachycardia with rapid pacing (0/4) (*Figure 4F*). In contrast, Nppa-/- (1/3) and Nppb-/- (1/3) hearts did develop ventricular tachycardia with rapid pacing (*Figure 4G and H*). These results show that hearts deficient in ANP or BNP have increased susceptibility to ventricular arrhythmias after acute stress.

3.6 ANP or BNP deficiency leads to reduced left ventricular myocardial cGMP

Our initial results suggested that ANP or BNP deficiency led to similar myocardial responses in both the unstressed and stressed states. Therefore, we wanted to determine if loss of ANP or BNP led to a compensatory increase in the expression of the remaining cardiac natriuretic peptide. We found that left ventricular myocardial tissue transcription of the cardiac natriuretic peptide genes was not increased in either Nppa-/- or Nppb-/- mice compared to wild-type mice at 1 or 4 months of age (*Figure 5A and B*). Interestingly, we found that Nppb-/- LV tissue actually had reduced transcription of the Nppa gene. There was no evidence of significant LV myocardial transcription of the non-cardiac natriuretic peptide, Nppc, in any of the groups (*Figure 5A and B*). Since transcription is only one mechanism for altering protein levels, we directly measured plasma levels of ANP and BNP peptides in mice from all three genotypes. Similar to the transcription data, there was no evidence that there was a compensatory increase in the remaining cardiac natriuretic peptide (*Figure 5C and D*). In addition, these ELISA-based assays confirmed that our Nppa-/- and Nppb-/- animals were indeed deficient in ANP and BNP peptides, respectively.

Since we could not detect a compensatory increase of the remaining cardiac natriuretic peptide in either Nppa-/- or Nppb-/- mice, we hypothesized that there would be abnormalities in myocardial cGMP levels. Indeed, both Nppa-/- and Nppb-/- LV myocardial tissue had reduced cGMP relative to WT controls (*Figure 5E*), suggesting that both peptides are necessary to maintain LV myocardial cGMP homeostasis in young animals. Taken together, we discovered that deficiency of either ANP or BNP does not lead to a compensatory increase of the remaining cardiac natriuretic peptide, resulting in a net reduction in LV myocardial cGMP levels.

3.7 Cardiac natriuretic peptides regulate cardiomyocyte CREB phosphorylation, and CREB inhibition sensitizes the heart to stress-induced ventricular arrhythmias

In contrast to the normal 6-month survival in our Mybpc3-/- model deficient in either ANP or BNP, an earlier study showed significantly decreased survival in a different murine model of dilated cardiomyopathy deficient in ANP.[39] The dilated cardiomyopathy model utilized in that study was induced by the transgenic overexpression of a dominant negative form of cAMP response element-binding protein (CREB S133A) in cardiomyocytes. Therefore, we hypothesized that deficiency of cardiac natriuretic peptides may lead to alterations in myocardial CREB S133

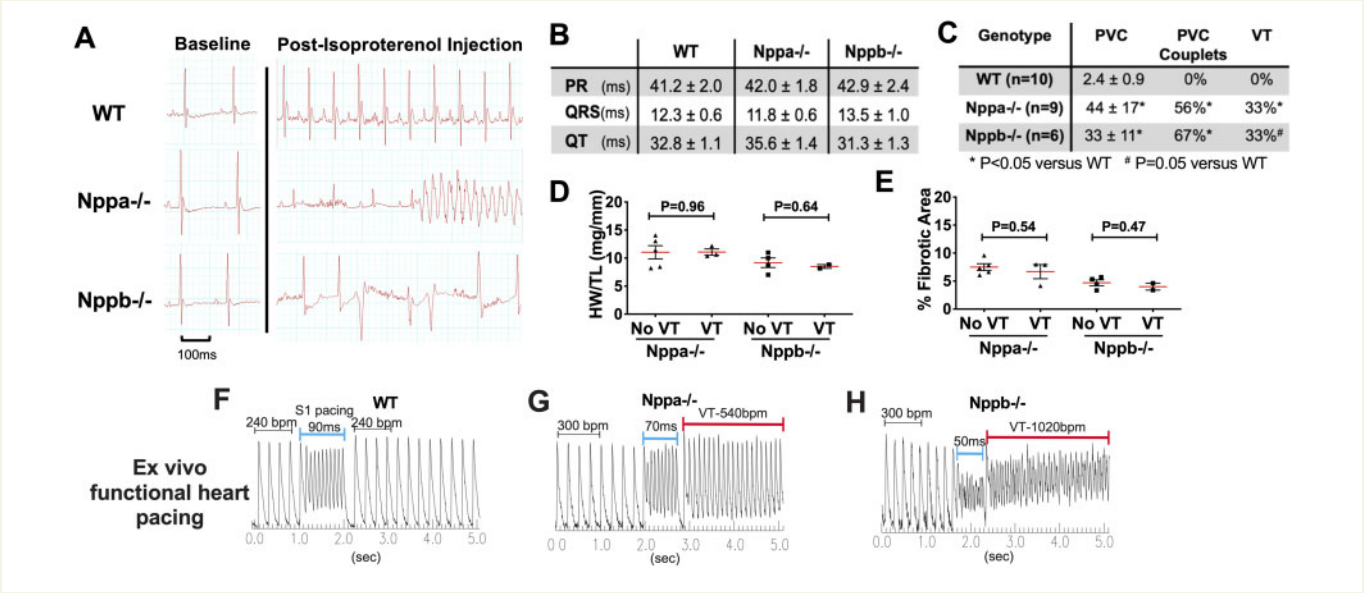

Figure 4 ANP or BNP deficiency increases susceptibility to ventricular arrythmias following acute stress. Six-month-old mice underwent continuous EKG monitoring. Baseline EKGs were obtained, after which the mice were injected with 1.5 mg/kg of isoproterenol. (*A*) Representative electrocardiograms (EKGs) before or after administration of isoproterenol (1.5 mg/kg) to WT ($N = 10$), Nppa-/- ($N = 9$), and Nppb-/- ($N = 6$) mice. The post-isoproterenol EKG strips for Nppa-/- and Nppb-/- mice show sustained (Nppa-/-) and non-sustained (Nppb-/-) ventricular tachycardia, respectively. (*B*) Baseline EKG measurements prior to isoproterenol injection. (*C*) The number of premature ventricular contractions (PVCs) per animal (mean ± SEM), the percentage of animals with PVC couplets, and the percentage of animals with sustained or non-sustained ventricular tachycardia (VT) after administration of isoproterenol. (*D*) Comparison of heart weight to tibial length (HW/TL, in mg/mm) in mice which did and did not experience VT, grouped by genotype ($N = 2$–5/group). (*E*) Comparison of per cent LV fibrotic area between mice which did and did not experience VT, grouped by genotype ($N = 2$–5/group). (*F–H*) Representative calcium transient images of WT ($N = 4$), Nppa-/- ($N = 3$), and Nppb-/- ($N = 3$) *ex vivo* hearts before and after rapid pacing. Student's *t*-test used to assess means between two groups. Data shown as means ± SEM. Chi-square test was used to assess categorical data.

phosphorylation (pCREB^{S133}), which could explain the increased mortality in the previous study. Interestingly, we confirmed significantly reduced pCREB^{S133} in both Nppa-/- and Nppb-/- LV tissue, with no change in overall CREB protein expression (*Figure 6A and B*).

Next, we evaluated the expression of inducible cAMP early repressor (ICER) whose expression is primarily regulated by CREB through a series of cAMP-responsive promoter elements.[40] We found ICER protein expression was significantly decreased in ANP- or BNP-deficient LV tissue compared to WT, confirming that decreased pCREB^{S133} is associated with reduced expression of a well-validated CREB target (*Figure 6C*).

However, it remained unclear if ANP or BNP could directly alter pCREB^{S133} in cardiomyocytes and if this signalling pathway was conserved in humans. Therefore, we exposed two genetically distinct human-induced pluripotent stem cell-derived cardiomyocyte lines (hiPS-CM) to ANP, BNP, or cGMP and measured pCREB^{S133} expression. We found that ANP, BNP, or cGMP induced a robust phosphorylation of CREB^{S133} in human cardiomyocytes and the response was similar in both genetically distinct hiPS-CM lines (*Figure 6D–F*).

Next, we wanted to determine if impaired CREB signalling contributes to the stress-induced ventricular arrhythmias detected in the ANP- and BNP-deficient animals. We found that selective pharmacological inhibition of CREB signalling over 16 days sensitized wild-type mice to isoproterenol-induced ventricular arrhythmias (*Figure 6G and H*). Selective CREB inhibition did not have any measurable effect on baseline EKG intervals, LV structure, or LV function (Supplementary material online, *Figure S4A–E*). These data demonstrate that selective CREB inhibition sensitizes the heart to stress-induced ventricular arrhythmias.

3.8 Cardiac natriuretic peptides regulate cardiomyocyte CREB^{S133} through a PKG1 and p38 MAPK pathway

Next, we sought to determine which kinases were regulating ANP and BNP effect on pCREB^{S133}. Therefore, we pre-treated the hiPS-CM with selective kinase inhibitors for PKG (KT5823), ERK1/2 (GDC-0994), and p38 MAPK (SB203580). Inhibition of PKG1 and PKG2 with KT5823 could prevent the ANP-induced phosphorylation of CREB^{S133} (*Figure 7A*). However, we also discovered that selective inhibition of p38 MAPK with SB203580 could also prevent phosphorylation of CREB^{S133} (*Figure 7A*). ERK 1/2 inhibition with GDC-0994 had no effect on pCREB^{S133} (*Figure 7A*). We then confirmed that ANP, BNP, and cGMP could induce the phosphorylation of p38 MAPK and that this phosphorylation could be prevented by selective inhibition of PKG or p38 MAPK (*Figure 7B*). Lastly, we confirmed that direct inhibition of CREB had no effect on p38 MAPK phosphorylation (Supplementary material online, *Figure S5A*).

Subsequently, we confirmed that PKG1 was transducing the signal between the natriuretic peptides and p38 MAPK and pCREB^{S133}. First, we successfully knocked down expression of PKG1 protein using siRNA in iPS-CM (*Figure 7C*). We then showed that the ANP-induced phosphorylation of both p38 MAPK and CREB^{S133} was significantly reduced in the absence of PKG1 (*Figure 7D–F*).

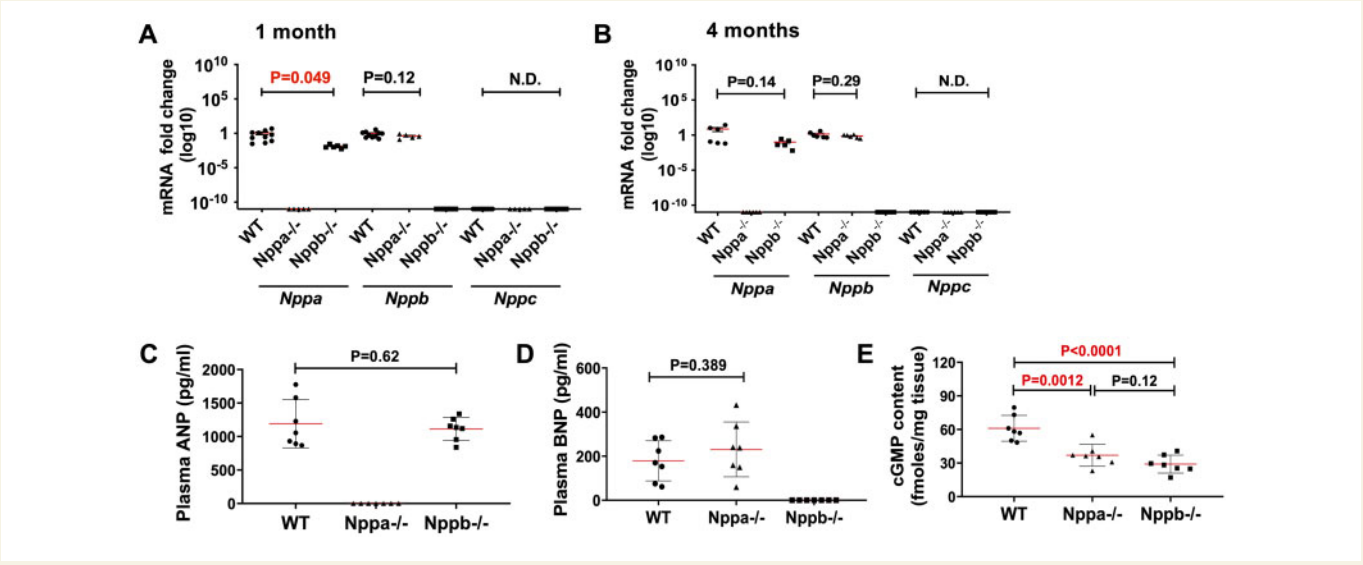

Figure 5 ANP or BNP deficiency leads to reduced left ventricular myocardial cGMP. (*A*) Measurement of Nppa, Nppb, and Nppc gene expression in 1-month-old WT ($N = 10$), Nppa-/- ($N = 5$), and Nppb-/- ($N = 6$) left ventricular myocardial tissue. The genes of interest were normalized to Rpl32 expression. Fold changes are shown in log10 value. Welch's *t*-test used to assess means between two groups. (*B*) Measurement of Nppa, Nppb, and Nppc gene expression in four-month-old WT ($N = 6$), Nppa-/- ($N = 6$), and Nppb-/- ($N = 5$) left ventricular myocardial tissue. The genes of interest were normalized to Rpl32 expression. Fold changes are shown in log10 value. Welch's *t*-test used to assess means between two groups. (*C*) Plasma ANP levels (pg/mL) in 1-month-old WT, Nppa-/-, and Nppb-/- animals ($N = 7$/group). (*D*) Plasma BNP levels (pg/ml) in 1-month-old WT, Nppa-/-, and Nppb-/- animals ($N = 7$/group). (*E*) Left ventricular myocardial cyclic guanine monophosphate (cGMP) levels (fmoles/mg tissue) in one-month-old WT, Nppa-/-, and Nppb-/- mice ($N = 7$/group). Student's *t*-test used to assess means between two groups. Data shown as means ± SEM.

Having established that NPs could regulate p38 MAPK *in vitro*, we then examined if ANP- and BNP-deficient mice had alterations in p38 MAPK phosphorylation in LV myocardial tissue. Indeed, we observed a significant reduction in p38 MAPK phosphorylation in LV myocardial tissue from Nppa-/- and Nppb-/- mice compared to WT mice (*Figure 7G*).

4. Discussion

To isolate the effect of cardiac NP deficiency on myocardial physiology, we directly compared ANP- and BNP-deficient murine models using matching experimental conditions and genetic backgrounds. We found that ANP or BNP deficiency sensitized animals to sudden death and ventricular arrhythmias after acute myocardial stress. This led us to discover that cardiac natriuretic peptides regulate cardiomyocyte CREB signalling through a cGMP-PKG1-p38 MAPK mechanism and deficiencies in this pathway lead to stress-induced ventricular arrhythmias.

4.1 A reduction in ANP or BNP leads to myocardial cGMP deficiency

To our knowledge, ours is the first work to directly compare ANP deficiency and BNP deficiency under identical genetic backgrounds and experimental conditions. Our work provides new insights into the molecular consequences of NP deficiency. We demonstrated that deficiency of either ANP or BNP is sufficient to cause reductions in myocardial cGMP, an important second messenger which plays a central role in regulating key signalling pathways.[9] We observed no increase in LV myocardial transcription or circulating plasma levels of the remaining NP in our ANP- or BNP-deficient animals less than 4 months of age. This is in contrast to embryonic heart development where ANP and BNP have more redundant functions in early cardiac morphogenesis.[41] It will be important to determine if the paracrine and endocrine responses to ANP or BNP deficiency are modified with aging. In conclusion, ANP or BNP deficiency in the mammalian heart leads to a reduction in LV myocardial cGMP levels.

4.2 Cardiac natriuretic peptides modulate CREB signalling

It remained unclear how cGMP reduction in ANP- and BNP-deficient mice modified cardiomyocyte signalling pathways. We identified a unique role for ANP and BNP signalling through cGMP and PKG1 in regulating CREB signalling utilizing both murine models and human-derived cardiomyocytes. CREB was initially identified as a target of protein kinase A that was phosphorylated at serine 133, and this phosphorylation event facilitated the binding of CREB to cAMP response element (CRE) sites in DNA to regulate gene transcription.[42,43] Since that initial discovery, it has also been reported that other kinases such as calcium calmodulin-dependent protein kinases can also phosphorylate $CREB^{S133}$ to regulate its transcriptional activity.[44] The importance of CREB in myocardial biology has been highlighted in multiple studies that either overexpressed a dominant negative form of CREB in cardiomyocytes or the selective ablation of CREB in cardiomyocytes. A murine model overexpressing a dominant negative CREB isoform ($CREB^{S133A}$) in cardiomyocytes develops dilated cardiomyopathy with a significant reduction in 6-month survival.[45] When this model is crossed with ANP-deficient mice, the resulting offspring develop a more aggressive form of cardiomyopathy and die at an earlier age.[39] Our discovery that ANP or BNP deficiency

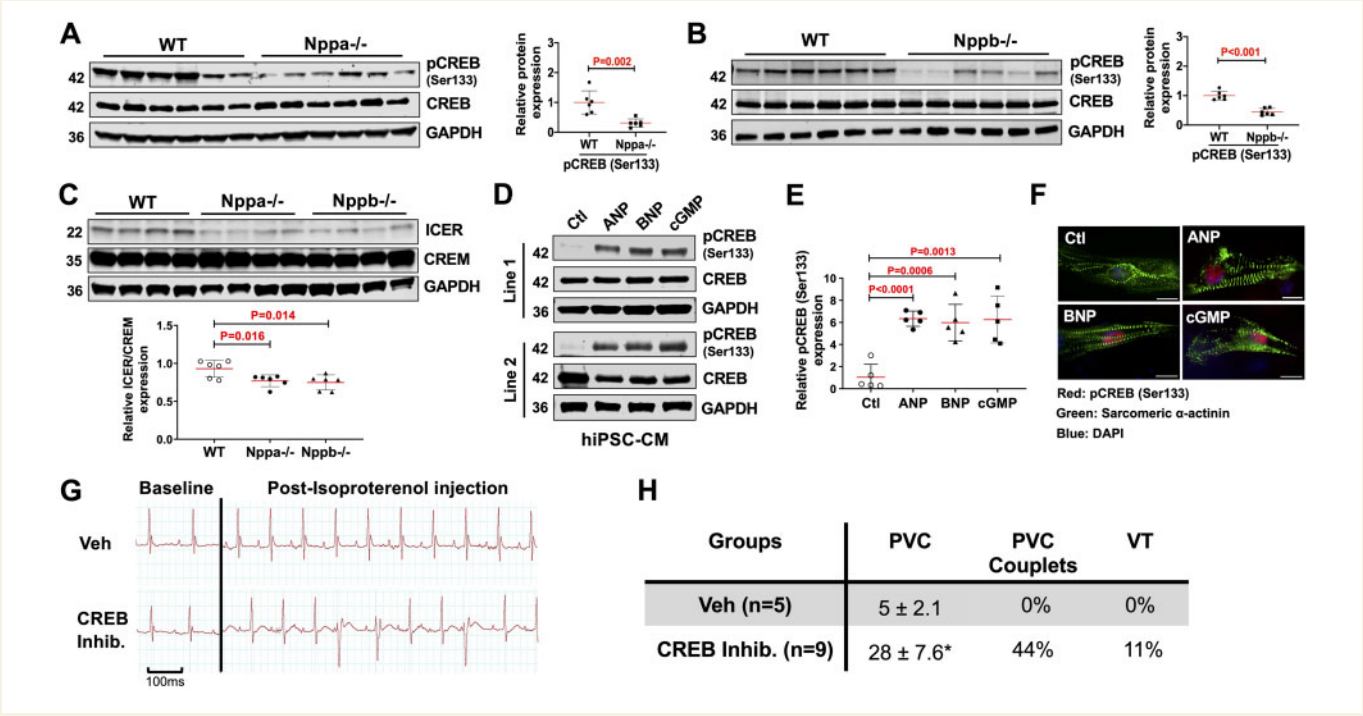

Figure 6 Cardiac natriuretic peptides regulate cardiomyocyte CREB phosphorylation and CREB inhibition sensitizes the heart to stress-induced ventricular arrhythmias. (*A*) Western blot of pCREB (Ser133) and total CREB from WT and Nppa-/- myocardial tissue. GAPDH used as loading control. Relative quantification pCREB from WT and Nppa-/- myocardial tissue normalized to total CREB ($N = 6$/group). (*B*) Western blot of pCREB (Ser133) and total CREB from WT and Nppb-/- myocardial tissue. Relative quantification pCREB from WT and Nppb-/- myocardial tissue normalized to total CREB ($N = 6$/group). (*C*) Representative western blot of inducible cAMP early repressor (ICER) and cAMP responsive element modulator (CREM) in WT, Nppa-/-, and Nppb-/- myocardial tissue. Relative quantification of ICER from WT, Nppa-/-, and Nppb-/- myocardial tissue normalized to CREM ($N = 6$/group). (*D*) Representative western blot of pCREB (Ser133) and total CREB in two different human-induced pluripotent-derived cardiomyocyte lines (hiPS-CM) exposed to ANP (0.1 μM), BNP (0.1 μM), or cGMP (0.1 μM) for 2 h. (*E*) Relative quantification of pCREB (Ser133) expression from hiPS-CMs normalized to total CREB ($N = 5$/group). (*F*) Representative immunofluorescence staining of pCREB(Ser133) (red) from Ctl, ANP, BNP, or cGMP-exposed hiPS-CMs. Sarcomeric α-actinin staining (green), nuclei labelled by DAPI (blue). Scale bars, 5 μm. (*G*) Representative electrocardiograms (EKG) before (baseline) and after isoproterenol administration in wild-type mice exposed to vehicle (Veh) or the selective CREB inhibitor (666-15, 10 mg/kg/day) for 16 days. (*H*) The number of premature ventricular contractions (PVCs) per animal (mean ± SEM), the percentage of animals with PVC couplets, and the percentage of animals with sustained or non-sustained ventricular tachycardia (VT) after administration of isoproterenol. *$P < 0.05$ CREB inhibitor vs. vehicle. Student's *t*-test used to assess means between two groups. Data shown as means ± SEM. Chi-square test was used to assess categorical data.

alone is associated with myocardial CREB^{S133} hypophosphorylation provides mechanistic insight into why the dominant negative CREB mice deficient in ANP had a more accelerated cardiomyopathy phenotype. In contrast to the transgenic overexpression of CREB^{S133A}, the cardiomyocyte deletion of CREB is not reported to cause an overt cardiomyopathy.[46] However, these mice do develop changes in cardiac electrophysiology with increased action potential duration and alterations in multiple cardiomyocyte ion channel proteins.[47] The cardiac phenotypic differences between transgenic overexpression of CREB^{S133A} and cardiomyocyte deletion of CREB may be explained by the fact that CREB forms heterodimers with other related transcription factors, such as ATF1 and CREM.[48,49] Therefore, a phosphorylation resistant or hypophosphorylated form of CREB may alter CREB regulated transcription differently than a complete loss of CREB protein. Our data shows that alterations in ANP or BNP levels lead to changes in cardiomyocyte CREB signalling, suggesting that these peptides can act in a paracrine fashion to modulate cardiomyocyte transcriptional pathways in both normal and disease states.

4.3 ANP or BNP deficiency predisposes to sudden death and ventricular arrhythmias following acute myocardial stress

An interesting discovery in our study was that the acute increase in LV afterload by TAC in ANP- and BNP-deficient mice resulted in early sudden death. Despite only mild myocardial structural changes, these mice demonstrated a 30–50% rate of sudden death in the 5 days following TAC. This mortality was present in both male and female mice, with no difference in the pre-TAC LV structure or function between survivors and sudden death groups. In addition, there was no evidence of infection or intrathoracic bleeding as a cause of death in these mice. We hypothesized that the sudden death was arrhythmogenic in nature and was initiated by acute myocardial stress. This was validated by our experiments showing that *in vivo* administration of isoproterenol or *ex vivo* rapid pacing in ANP- or BNP-deficient animals induced ventricular tachycardia. Pharmacological inhibition of CREB phenocopied the stress induced ventricular arrhythmias detected in ANP- or BNP-deficient animals. Therefore, our results suggest that reduced CREB signalling is a major

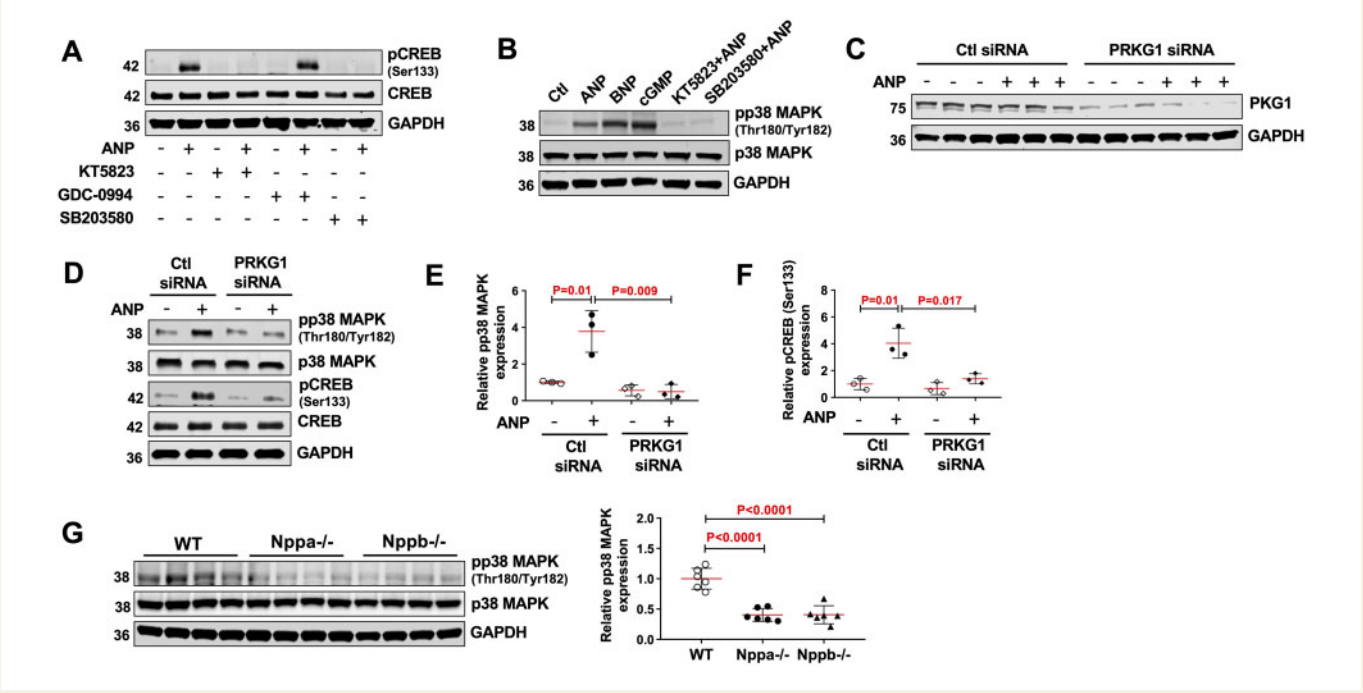

Figure 7 Cardiac natriuretic peptides regulate cardiomyocyte CREB^{S133} through a PKG1 and p38 MAPK pathway. (*A*) iPS-CMs were exposed to either vehicle (-), PKG inhibitor (KT5823, 0.1 μM), ERK1/2 inhibitor (GDC-0994, 0.1 μM), or p38 MAPK inhibitor (SB203580, 0.1 μM) for 2 h and then exposed to ANP for an additional 2 h, and a western blot was performed for pCREB (Ser133). GAPDH used as loading control ($N = 3$/group). (*B*) Western blot of phos-p38 MAPK (Thr180/Tyr182) and total p38 MAPK in hiPS-CM exposed to ANP, BNP, cGMP, KT5823 + ANP, or SB203520 + ANP ($N = 3$/group). (*C*) iPS-CMs were exposed to either scrambled control siRNA or PRKG1 targeting siRNA. Knockdown efficacy was assessed by western blot of PKG1 protein after 2 h ANP exposure of the iPS-CM lines. GAPDH used as loading control ($N = 3$/group). (*D*) Representative western blot of phos-p38 MAPK (Thr180/Tyr182), total p38 MAPK, pCREB (Ser133), and total CREB from the control or PRKG1 siRNA-treated group described above. (*E*) Relative quantification of phos-p38 MAPK from the iPS-CM exposed to control siRNA or PRKG1 siRNA and then exposed to ANP. Phos-p38 MAPK was normalized to total p38 MAPK ($N = 3$/group). (*F*) Relative quantification of pCREB (Ser133) from the iPS-CM exposed to control siRNA or PRKG1 siRNA and then exposed to ANP. pCREB (Ser133) was normalized to total CREB ($N = 3$/group). (*G*) Western blot of phos-p38 MAPK (Thr180/Tyr182) and total p38 MAPK in WT, Nppa-/-, and Nppb-/- myocardial tissue. Relative quantification phos-p38 MAPK from WT, Nppa-/-, and Nppb-/- myocardial tissue normalized to total p38 MAPK ($N = 6$/group). Student's *t*-test used to assess means between two groups. Data shown as means ± SEM.

contributor to the arrhythmia phenotypes detected in the NP-deficient animals. Importantly, it has been previously reported that a reduction of cardiomyocyte CREB signalling leads to alterations in multiple cardiomyocyte ion channels.[47,50,51]

Interestingly, it was reported that Npr1 null male mice had increased spontaneous sudden death in the F2 generation of a 129-C57BL/6 mice mixed genetic background.[52] In contrast to our ANP- or BNP-deficient mice, the Npr1 mice in that study had very high levels of hypertension and LV hypertrophy. Of note, the same investigators no longer detected sudden death in future generations of Npr1 mice which they concluded was secondary to genetic drift in the mixed 129-C57BL/6 background.[53] In contrast to this earlier study, we did not detect spontaneous sudden death in ANP- or BNP-deficient mice in a C57BL/6J genetic background. However, ANP- or BNP-deficient animals did have increased sudden death or ventricular arrhythmias after multiple different forms of acute myocardial stress. Taken together, the data from the earlier Npr1 studies and our study show that perturbations in myocardial NP signalling leads to increased sudden death and also raise the possibility that genetic modifiers may influence this phenotypic response. Our elucidation of a cardiac natriuretic peptide-PKG1-p38 MAPK-CREB signalling pathway in cardiomyocytes provides potential mechanistic insight into the reduction of sudden death reported in human heart failure patients treated with the neprilysin inhibitor sacubitril/valsartan combination drug which increases circulating natriuretic peptide levels.[24]

4.4 Cardiomyocyte p38 MAPK signalling is activated by ANP and BNP

After identification that ANP and BNP could modify CREB^{S133} phosphorylation, we elucidated that ANP and BNP were acting through PKG1 to phosphorylate p38 MAPK and this regulated CREB^{S133} phosphorylation. Importantly, we also found that chronic deficiency of ANP or BNP led to reduced phosphorylation of p38 MAPK in the left ventricular myocardium of our murine models. These discoveries are important since p38 MAPK signalling has been shown to be essential in the cardiomyocyte response to multiple different pathological stressors.[54] For example, genetic deletion of p38α in cardiomyocytes led to no detectable myocardial changes at baseline but caused increased pathological remodelling after TAC and a 4 fold increase in sudden death in the 7-day period following the procedure.[55] In addition, cardiomyocyte overexpression of a dominant negative p38α isoform resulted in increased myocardial hypertrophy in both the unstressed and stressed state.[56] In contrast, other research suggested that p38 MAPK overactivation

was also deleterious, particularly in atherosclerosis and post-infarction myocardial remodelling.[57] However, chemical inhibition of p38 MAPK after myocardial infarction failed to improve outcomes in humans.[58] Overall, it would appear that a chronic reduction in myocardial p38 MAPK activity contributes to adverse responses to pathological myocardial stress. Our results demonstrate that ANP and BNP are capable of increasing cardiomyocyte p38 MAPK activity and may be one potential mechanism by which cardiac NP's protect the myocardium from stress and improve myocardial remodelling in heart failure.

4.5 ANP and BNP deficiency and LV remodelling

In the unstressed state, ANP- and BNP-deficient animals demonstrated distinct LV structural changes in comparison with WT mice. At younger ages, ANP-deficient animals had increased LV hypertrophy and fibrosis, consistent with prior research.[25,27,59,60] BNP-deficient mice displayed mild LV hypertrophy and LV dilation on phenotyping at 60 days of age, and these changes did not increase substantially with aging. Interestingly, previous work described increased myocardial fibrosis in BNP-deficient mice, which we did not observe at 6 months of age.[28] Genetic background may be one possible reason for the phenotypic difference, since the earlier study used 129/Sv mice and our study utilized C57BL/6J mice. In contrast to the unstressed state, we did see a trend of increased LV myocardial fibrosis in BNP-deficient mice at 6 weeks post-TAC but it did not meet statistical significance ($P = 0.09$). In addition, it is possible that other environmental factors independent of mouse genetic background contributed to the increased myocardial fibrosis reported in the earlier study. We did not observe the severe cardiac hypertrophy that is reported in mice deficient in Npr1, which is the primary receptor for ANP and BNP.[52] Importantly, Npr1-deficient mice have significant hypertension which contributes to the LV hypertrophic response, while our ANP- and BNP-deficient mice did not have significant differences in systolic blood pressure compared to WT mice. In addition, a complete loss of Npr1 activity would be predicted to have a more profound effect on cellular cGMP production compared to loss of either ANP or BNP alone.

Similar to the unstressed heart, we did not see a dramatic effect of ANP or BNP deficiency in the LV remodelling response in either acute (TAC) or chronic (Mybpc3-/-) myocardial stress. We were surprised by these findings, but the results were consistent between both forms of myocardial stress investigated. It is possible that the high rate of sudden death in the ANP- and BNP-deficient TAC groups may have created a selection bias. However, the pre-TAC phenotyping did not detect LV structural differences between survivors and non-survivors. Likewise, the chronic form of myocardial stress we utilized (Mybpc3 deficiency) does not model other forms of genetic or acquired dilated cardiomyopathy. Therefore, ANP or BNP deficiency may have unique effects on LV remodelling depending on the primary cause of the chronic cardiomyopathy. Overall, our results indicate that ANP and BNP are both necessary to maintain normal LV myocardial cGMP levels but deficiency of ANP or BNP alone has only mild effects on LV remodelling in the unstressed and stressed states.

5. Conclusion

We performed a direct comparison of ANP to BNP deficiency in similar environments and genetic backgrounds to better understand how these peptides regulate cardiomyocyte function and LV remodelling. ANP or BNP deficiency had mild effects on LV structural remodelling but significantly increased the rate of sudden death and ventricular arrhythmias following acute myocardial stress. We discovered that ANP and BNP regulate cardiomyocyte p38 MAPK and $CREB^{S133}$ phosphorylation through a cGMP–PKG1 pathway and impaired CREB signalling is a primary mechanism by which natriuretic peptide-deficient states sensitize the heart to stress-induced ventricular arrhythmias. These findings are particularly important given the expanding role of modulating natriuretic peptide levels to reduce mortality in human heart failure patients.

Supplementary material

Supplementary material is available at *Cardiovascular Research* online.

Conflict of interest: none declared.

Funding

This study was supported by National Institutes of Health R01HL136824 to J.R.B. and Vanderbilt Medical Scholar Program funding to E.J.H.

Data availability

The data underlying this article are available in the article and in its online supplementary material.

References

1. Dietz JR. Mechanisms of atrial natriuretic peptide secretion from the atrium. *Cardiovasc Res* 2005;**68**:8–17.
2. Kinnunen P, Vuolteenaho O, Ruskoaho H. Mechanisms of atrial and brain natriuretic peptide release from rat ventricular myocardium: effect of stretching. *Endocrinology* 1993;**132**:1961–1970.
3. Burnett JC Jr, Kao PC, Hu DC, Heser DW, Heublein D, Granger JP, Opgenorth TJ, Reeder GS. Atrial natriuretic peptide elevation in congestive heart failure in the human. *Science* 1986;**231**:1145–1147.
4. Brunner-La Rocca HP, Kaye DM, Woods RL, Hastings J, Esler MD. Effects of intravenous brain natriuretic peptide on regional sympathetic activity in patients with chronic heart failure as compared with healthy control subjects. *J Am Coll Cardiol* 2001;**37**:1221–1227.
5. de Bold AJ, Borenstein HB, Veress AT, Sonnenberg H. A rapid and potent natriuretic response to intravenous injection of atrial myocardial extract in rats. *Life Sci* 1981;**28**:89–94.
6. Kita T, Kida O, Kato J, Nakamura S, Eto T, Minamino N, Kangawa K, Matsuo H, Tanaka K. Natriuretic and hypotensive effects of brain natriuretic peptide (BNP) in spontaneously hypertensive rats. *Life Sci* 1989;**44**:1541–1545.
7. Potter LR, Yoder AR, Flora DR, Antos LK, Dickey DM. Natriuretic peptides: their structures, receptors, physiologic functions and therapeutic applications. *Handb Exp Pharmacol* 2009;**191**:341–366.
8. Zois NE, Bartels ED, Hunter I, Kousholt BS, Olsen LH, Goetze JP. Natriuretic peptides in cardiometabolic regulation and disease. *Nat Rev Cardiol* 2014;**11**:403–412.
9. Tsai EJ, Kass DA. Cyclic GMP signaling in cardiovascular pathophysiology and therapeutics. *Pharmacol Ther* 2009;**122**:216–238.
10. Suga S, Nakao K, Hosoda K, Mukoyama M, Ogawa Y, Shirakami G, Arai H, Saito Y, Kambayashi Y, Inouye K. Receptor selectivity of natriuretic peptide family, atrial natriuretic peptide, brain natriuretic peptide, and C-type natriuretic peptide. *Endocrinology* 1992;**130**:229–239.
11. Johns DG, Ao Z, Heidrich BJ, Hunsberger GE, Graham T, Payne L, Elshourbagy N, Lu Q, Aiyar N, Douglas SA. Dendroaspis natriuretic peptide binds to the natriuretic peptide clearance receptor. *Biochem Biophys Res Commun* 2007;**358**:145–149.
12. Potter LR. Natriuretic peptide metabolism, clearance and degradation. *FEBS J* 2011;**278**:1808–1817.
13. Maack T, Suzuki M, Almeida FA, Nussenzveig D, Scarborough RM, McEnroe GA, Lewicki JA. Physiological role of silent receptors of atrial natriuretic factor. *Science* 1987;**238**:675–678.

14. Koehn JA, Norman JA, Jones BN, LeSueur L, Sakane Y, Ghai RD. Degradation of atrial natriuretic factor by kidney cortex membranes: isolation and characterization of the primary proteolytic product. *J Biol Chem* 1987;**262**:11623–11627.
15. Newton-Cheh C, Larson MG, Vasan RS, Levy D, Bloch KD, Surti A, Guiducci C, Kathiresan S, Benjamin EJ, Struck J, Morgenthaler NG, Bergmann A, Blankenberg S, Kee F, Nilsson P, Yin X, Peltonen L, Vartiainen E, Salomaa V, Hirschhorn JN, Melander O, Wang TJ. Association of common variants in NPPA and NPPB with circulating natriuretic peptides and blood pressure. *Nat Genet* 2009;**41**:348–353.
16. Hodgson-Zingman DM, Karst ML, Zingman LV, Heublein DM, Darbar D, Herron KJ, Ballew JD, de Andrade M, Burnett JC, Jr., Olson TM. Atrial natriuretic peptide frameshift mutation in familial atrial fibrillation. *N Engl J Med* 2008;**359**:158–165.
17. Rubattu S, Bigatti G, Evangelista A, Lanzani C, Stanzione R, Zagato L, Manunta P, Marchitti S, Venturelli V, Bianchi G, Volpe M, Stella P. Association of atrial natriuretic peptide and type a natriuretic peptide receptor gene polymorphisms with left ventricular mass in human essential hypertension. *J Am Coll Cardiol* 2006;**48**: 499–505.
18. Gupta DK, de Lemos JA, Ayers CR, Berry JD, Wang TJ. Racial differences in natriuretic peptide levels: the Dallas Heart Study. *JACC Heart Fail* 2015;**3**:513–519.
19. Wang T, Larson MG, Levy D, Benjamin EJ, Leip EP, Wilson PWF, Vasan RS. Impact of obesity on plasma natriuretic peptide levels. *Circulation* 2004;**109**:594–600.
20. Maisel AS, Krishnaswamy P, Nowak RM, McCord J, Hollander JE, Duc P, Omland T, Storrow AB, Abraham WT, Wu AHB, Clopton P, Steg PG, Westheim A, Knudsen CW, Perez A, Kazanegra R, Herrmann HC, McCullough PA; Breathing Not Properly Multinational Study Investigators. Rapid measurement of B-type natriuretic peptide in the emergency diagnosis of heart failure. *N Engl J Med* 2002;**347**: 161–167.
21. Reginauld SH, Cannone V, Iyer S, Scott C, Bailey K, Schaefer J, Chen Y, Sangaralingham SJ, Burnett JC Jr. Differential regulation of ANP and BNP in acute decompensated heart failure: deficiency of ANP. *JACC Heart Fail* 2019;**7**:891–898.
22. Hawkridge AM, Heublein DM, Bergen HR 3rd, Cataliotti A, Burnett JC Jr, Muddiman DC. Quantitative mass spectral evidence for the absence of circulating brain natriuretic peptide (BNP-32) in severe human heart failure. *Proc Natl Acad Sci USA* 2005; **102**:17442–17447.
23. Niederkofler EE, Kiernan UA, O'Rear J, Menon S, Saghir S, Protter AA, Nelson RW, Schellenberger U. Detection of endogenous B-type natriuretic peptide at very low concentrations in patients with heart failure. *Circ Heart Fail* 2008;**1**:258–264.
24. McMurray JJ, Packer M, Desai AS, Gong J, Lefkowitz MP, Rizkala AR, Rouleau JL, Shi VC, Solomon SD, Swedberg K, Zile MR; Investigators PH and Committees. Angiotensin-neprilysin inhibition versus enalapril in heart failure. *N Engl J Med* 2014; **371**:993–1004.
25. John SW, Krege JH, Oliver PM, Hagaman JR, Hodgin JB, Pang SC, Flynn TG, Smithies O. Genetic decreases in atrial natriuretic peptide and salt-sensitive hypertension. *Science* 1995;**267**:679–681.
26. John SW, Veress AT, Honrath U, Chong CK, Peng L, Smithies O, Sonnenberg H. Blood pressure and fluid-electrolyte balance in mice with reduced or absent ANP. *Am J Physiol* 1996;**271**:R109–R114.
27. Feng JA, Perry G, Mori T, Hayashi T, Oparil S, Chen YF. Pressure-independent enhancement of cardiac hypertrophy in atrial natriuretic peptide-deficient mice. *Clin Exp Pharmacol Physiol* 2003;**30**:343–349.
28. Tamura N, Ogawa Y, Chusho H, Nakamura K, Nakao K, Suda M, Kasahara M, Hashimoto R, Katsuura G, Mukoyama M, Itoh H, Saito Y, Tanaka I, Otani H, Katsuki M. Cardiac fibrosis in mice lacking brain natriuretic peptide. *Proc Natl Acad Sci USA* 2000;**97**:4239–4244.
29. Nixon BR, Williams AF, Glennon MS, de Feria AE, Sebag SC, Baldwin HS, Becker JR. Alterations in sarcomere function modify the hyperplastic to hypertrophic transition phase of mammalian cardiomyocyte development. *JCI Insight* 2017;**2**:e90656.
30. Zhou J, Lal H, Chen X, Shang X, Song J, Li Y, Kerkela R, Doble BW, MacAulay K, DeCaul M, Koch WJ, Farber J, Woodgett J, Gao E, Force T. GSK-3alpha directly regulates beta-adrenergic signaling and the response of the heart to hemodynamic stress in mice. *J Clin Invest* 2010;**120**:2280–2291.
31. Merentie M, Lipponen JA, Hedman M, Hedman A, Hartikainen J, Huusko J, Lottonen-Raikaslehto L, Parviainen V, Laidinen S, Karjalainen PA, Yla-Herttuala S. Mouse ECG findings in aging, with conduction system affecting drugs and in cardiac pathologies: development and validation of ECG analysis algorithm in mice. *Physiol Rep* 2015;**3**: e12639.
32. Zhang Y, Wu J, King JH, Huang CL, Fraser JA. Measurement and interpretation of electrocardiographic QT intervals in murine hearts. *Am J Physiol Heart Circ Physiol* 2014;**306**:H1553–H1557.
33. Curtis MJ, Hancox JC, Farkas A, Wainwright CL, Stables CL, Saint DA, Clements-Jewery H, Lambiase PD, Billman GE, Janse MJ, Pugsley MK, Ng GA, Roden DM, Camm AJ, Walker MJ. The Lambeth Conventions (II): guidelines for the study of animal and human ventricular and supraventricular arrhythmias. *Pharmacol Ther* 2013; **139**:213–248.
34. Xie F, Li BX, Kassenbrock A, Xue C, Wang X, Qian DZ, Sears RC, Xiao X. Identification of a potent inhibitor of CREB-mediated gene transcription with efficacious in vivo anticancer activity. *J Med Chem* 2015;**58**:5075–5087.
35. Choi BR, Salama G. Simultaneous maps of optical action potentials and calcium transients in guinea-pig hearts: mechanisms underlying concordant alternans. *J Physiol* 2000;**529 (pt. 1)**:171–188.
36. Salama G, Hwang SM. Simultaneous optical mapping of intracellular free calcium and action potentials from Langendorff perfused hearts. *Curr Protoc Cytom* 2009;**49**:12–17.
37. Burridge PW, Holmstrom A, Wu JC. Chemically defined culture and cardiomyocyte differentiation of human pluripotent stem cells. *Curr Protoc Hum Genet* 2015;**87**: 21–23.
38. Kadari A, Mekala S, Wagner N, Malan D, Koth J, Doll K, Stappert L, Eckert D, Peitz M, Matthes J, Sasse P, Herzig S, Brustle O, Ergun S, Edenhofer F. Robust generation of cardiomyocytes from human iPS cells requires precise modulation of BMP and WNT signaling. *Stem Cell Rev Rep* 2015;**11**:560–569.
39. Wang D, Gladysheva IP, Fan TH, Sullivan R, Houng AK, Reed GL. Atrial natriuretic peptide affects cardiac remodeling, function, heart failure, and survival in a mouse model of dilated cardiomyopathy. *Hypertension* 2014;**63**:514–519.
40. Molina CA, Foulkes NS, Lalli E, Sassone-Corsi P. Inducibility and negative autoregulation of CREM: an alternative promoter directs the expression of ICER, an early response repressor. *Cell* 1993;**75**:875–886.
41. Becker JR, Chatterjee S, Robinson TY, Bennett JS, Panakova D, Galindo CL, Zhong L, Shin JT, Coy SM, Kelly AE, Roden DM, Lim CC, MacRae CA. Differential activation of natriuretic peptide receptors modulates cardiomyocyte proliferation during development. *Development* 2014;**141**:335–345.
42. Montminy MR, Bilezikjian LM. Binding of a nuclear protein to the cyclic-AMP response element of the somatostatin gene. *Nature* 1987;**328**:175–178.
43. Gonzalez GA, Montminy MR. Cyclic AMP stimulates somatostatin gene transcription by phosphorylation of CREB at serine 133. *Cell* 1989;**59**:675–680.
44. Sheng M, Thompson MA, Greenberg ME. CREB: a Ca(2+)-regulated transcription factor phosphorylated by calmodulin-dependent kinases. *Science* 1991;**252**: 1427–1430.
45. Fentzke RC, Korcarz CE, Lang RM, Lin H, Leiden JM. Dilated cardiomyopathy in transgenic mice expressing a dominant-negative CREB transcription factor in the heart. *J Clin Invest* 1998;**101**:2415–2426.
46. Matus M, Lewin G, Stumpel F, Buchwalow IB, Schneider MD, Schutz G, Schmitz W, Muller FU. Cardiomyocyte-specific inactivation of transcription factor CREB in mice. *FASEB J* 2007;**21**:1884–1892.
47. Schulte JS, Seidl MD, Nunes F, Freese C, Schneider M, Schmitz W, Müller FU. CREB critically regulates action potential shape and duration in the adult mouse ventricle. *Am J Physiol Heart Circ Physiol* 2012;**302**:H1998–H2007.
48. Hurst HC, Totty NF, Jones NC. Identification and functional characterisation of the cellular activating transcription factor 43 (ATF-43) protein. *Nucleic Acids Res* 1991;**19**: 4601–4609.
49. Laoide BM, Foulkes NS, Schlotter F, Sassone-Corsi P. The functional versatility of CREM is determined by its modular structure. *EMBO J* 1993;**12**:1179–1191.
50. Huang H, Amin V, Gurin M, Wan E, Thorp E, Homma S, Morrow JP. Diet-induced obesity causes long QT and reduces transcription of voltage-gated potassium channels. *J Mol Cell Cardiol* 2013;**59**:151–158.
51. Ozgen N, Lau DH, Shlapakova IN, Sherman W, Feinmark SJ, Danilo P Jr, Rosen MR. Determinants of CREB degradation and KChIP2 gene transcription in cardiac memory. *Heart Rhythm* 2010;**7**:964–970.
52. Oliver PM, Fox JE, Kim R, Rockman HA, Kim HS, Reddick RL, Pandey KN, Milgram SL, Smithies O, Maeda N. Hypertension, cardiac hypertrophy, and sudden death in mice lacking natriuretic peptide receptor A. *Proc Natl Acad Sci USA* 1997;**94**: 14730–14735.
53. Knowles JW, Esposito G, Mao L, Hagaman JR, Fox JE, Smithies O, Rockman HA, Maeda N. Pressure-independent enhancement of cardiac hypertrophy in natriuretic peptide receptor A-deficient mice. *J Clin Invest* 2001;**107**:975–984.
54. Yokota T, Wang Y. p38 MAP kinases in the heart. *Gene* 2016;**575**:369–376.
55. Nishida K, Yamaguchi O, Hirotani S, Hikoso S, Higuchi Y, Watanabe T, Takeda T, Osuka S, Morita T, Kondoh G, Uno Y, Kashiwase K, Taniike M, Nakai A, Matsumura Y, Miyazaki J, Sudo T, Hongo K, Kusakari Y, Kurihara S, Chien KR, Takeda J, Hori M, Otsu K. p38alpha mitogen-activated protein kinase plays a critical role in cardiomyocyte survival but not in cardiac hypertrophic growth in response to pressure overload. *Mol Cell Biol* 2004;**24**:10611–10620.
56. Braz JC, Bueno OF, Liang Q, Wilkins BJ, Dai YS, Parsons S, Braunwart J, Glascock BJ, Klevitsky R, Kimball TF, Hewett TE, Molkentin JD. Targeted inhibition of p38 MAPK promotes hypertrophic cardiomyopathy through upregulation of calcineurin-NFAT signaling. *J Clin Invest* 2003;**111**:1475–1486.
57. Denise Martin E, De Nicola GF, Marber MS. New therapeutic targets in cardiology: p38 alpha mitogen-activated protein kinase for ischemic heart disease. *Circulation* 2012;**126**:357–368.
58. O'Donoghue ML, Glaser R, Cavender MA, Aylward PE, Bonaca MP, Budaj A, Davies RY, Dellborg M, Fox KA, Gutierrez JA, Hamm C, Kiss RG, Kovar F, Kuder JF, Im KA, Lepore JJ, Lopez-Sendon JL, Ophuis TO, Parkhomenko A, Shannon JB, Spinar J, Tanguay JF, Ruda M, Steg PG, Theroux P, Wiviott SD, Laws I, Sabatine MS, Morrow DA; LATITUDE-TIMI 60 Investigators. Effect of losmapimod on cardiovascular outcomes in patients hospitalized with acute myocardial infarction: a randomized clinical trial. *JAMA* 2016;**315**:1591–1599.

59. Franco V, Chen YF, Oparil S, Feng JA, Wang D, Hage F, Perry G. Atrial natriuretic peptide dose-dependently inhibits pressure overload-induced cardiac remodeling. *Hypertension* 2004;**44**:746–750.

60. Wang D, Oparil S, Feng JA, Li P, Perry G, Chen LB, Dai M, John SW, Chen YF. Effects of pressure overload on extracellular matrix expression in the heart of the atrial natriuretic peptide-null mouse. *Hypertension* 2003;**42**:88–95.

Translational perspective

Our study found that ANP or BNP deficiency leads to increased sudden death and ventricular arrhythmias after acute myocardial stress in murine models. We discovered that ANP and BNP act in a non-redundant fashion to maintain myocardial cGMP levels and uncovered a unique role for these peptides in regulating cardiomyocyte p38 MAPK and CREB signalling through a cGMP–PKG1 pathway. Importantly, this signalling pathway was conserved in human cardiomyocytes. This study provides mechanistic insight into how modulating natriuretic peptide levels in human heart failure patients reduces sudden death and mortality.